ASSESSING GEO AND LEO REPEATING CONJUNCTIONS USING HIGH FIDELITY BRUTE FORCE MONTE CARLO SIMULATIONS

Luis Baars*, Doyle Hall†, and Steve Casali‡

Probability of collision (P_c) estimates for Earth-orbiting satellites typically assume a temporally-isolated conjunction event. However, under certain conditions two objects may experience multiple high-risk close approach events over the course of hours or days. In these repeating conjunction cases, the P_c accumulates as each successive encounter occurs. The NASA Conjunction Assessment Risk Analysis team has updated its "brute force Monte Carlo" (BFMC) software to estimate such accumulating P_c values for repeating conjunctions. This study describes the updated BFMC algorithm and discusses the implications for conjunction risk assessment.

INTRODUCTION

The NASA Conjunction Assessment Risk Analysis (CARA) team estimates the probability of collision (P_c) for a specific set of high value, Earth-orbiting satellites. The CARA processing system first detects candidate close encounters involving high value assets up to ten days in advance using a screening-volume approach, based on the latest available satellite tracking data and orbit determination (OD) state and covariance solutions.[1,2]

For each conjunction, CARA assesses the collision risk using a set of established semi-analytical, and Monte Carlo P_c approximation methods.[3,4,5] Under certain circumstances, a satellite may experience multiple close approach events with another object over the course of hours or even days. For these "repeating" conjunctions, collision probability accumulates as each close approach event occurs. Many GEO satellites orbit within clusters (by mission design), so it follows that these closely-spaced objects experience a higher frequency of repeating conjunctions. GEO cluster objects can also experience long duration encounters due to their low relative velocities.[4] Repeating and long-duration encounters also occur at other orbit regimes.[6] Most widely-used semi-analytical P_c estimation methods only consider temporally-isolated, short-duration conjunctions.[4,5,7] One approach for assessing collision risk for repeating conjunctions would be to combine semi-analytical, single-encounter P_c estimates of multiple successive encounters in order to estimate a cumulative

---

* Conjunction Assessment Research Analyst, Omitron Inc., 555 E. Pikes Peak Ave, #205 Colorado Springs, CO 80903, USA.

† Senior Conjunction Assessment Research Scientist, Omitron Inc., 555 E. Pikes Peak Ave, #205 Colorado Springs, CO 80903, USA.

‡ Chief Astrodynamicist, Omitron Inc., 555 E. Pikes Peak Ave, #205 Colorado Springs CO 80903, USA.

P_c. However, this approach implicitly assumes that the repeating conjunctions are statistically independent events, and may yield inaccurate results, especially for repeating long-duration encounters that are closely spaced in time and effectively overlap or blend with one another.

CARA requires a P_c estimation method to assess collision risk for repeating conjunctions accurately. In a previous study,[7] the CARA team presented a "brute force Monte Carlo" (BFMC) method using Special Perturbations (SP) orbital propagation[8] within a Monte Carlo (MC) framework.[9] The BFMC algorithm is general enough to account for the accumulation of collision probability during a temporally-isolated conjunction, or throughout a series of repeating and/or long-duration encounters.[7] The previous version of the BFMC software, however, was only implemented to address temporally-isolated conjunctions. The updated BFMC implementation differs from the original by increasing the collision risk assessment period from a relatively short interval (that closely brackets the time of peak risk for a temporally-isolated encounter) to an extended duration (that can span multiple encounters).

When analyzing repeating conjunctions, this extended risk assessment period can begin as early as the most recent of the two OD epoch times for the primary and secondary satellites, and end several days later. Because of this, collisions in the MC simulation can be distributed over an extended, multi-orbit interval, much longer than the typical span (measured in seconds to minutes) for temporally-isolated conjunctions. Additionally, the collisions can be distributed in time in one of three characteristic ways:

1. They occur in brief "bursts" separated by regular intervals, producing a stair-step trend in cumulative P_c characterized by relatively long durations without a collision.

2. The collision bursts widen and blend together such that the P_c accumulates more steadily over the risk assessment interval.

3. There is a combination of the stair-step and blended P_c trends.

As will be shown later, a cumulative P_c plot can be used to visualize how risk increases throughout a repeating conjunction interaction, and assess if and when it may exceed an acceptable maximum-risk level for different missions. This paper describes recent updates to the BFMC algorithm in detail, presents cumulative P_c plots for various GEO and LEO repeating conjunction cases, and discusses the implications for future conjunction risk assessments.

THE BFMC ALGORITHM

This section presents a brief overview of the BFMC algorithm to provide context for the recent updates implemented for processing repeating conjunctions.

Original BFMC Algorithm

MC P_c estimation simulations can be computationally intensive because they require repeatedly performing the following steps:[7,10]

1. Sample the orbital state probability density functions (PDFs) of the primary and secondary satellites at some epoch.

2. Use the sampled states to propagate satellite state vectors throughout a risk assessment period, determining if the distance between the objects ever becomes less than a combined hard-body protection radius.

3. If the miss distance becomes less than the protection radius, register that a simulated collision has occurred.

These three steps together represent one BFMC sampling trial. Trials need to be repeated until enough simulated collisions (or "hits") have been registered to provide sufficiently accurate statistical results, which may require a large number of samples depending on the conjunction. (For instance, to estimate a collision probability to ~20% accuracy at a 95% confidence level typically requires ~100 hits[7] which in turn requires ~10^6 trials for an event that has $P_c = 10^{-4}$.) Step 2 requires significant computation, especially for complex propagation schemes[7,9] and when assessing collision risks accumulated over extended intervals.

The orbital state sampling in step 1 above can be performed in two distinctly different ways:[9]

- SP states can be sampled from PDFs estimated at the OD epochs for the primary and secondary satellites, and then propagated forward in time throughout the risk assessment period.
- Alternatively, equinoctial states can be sampled from PDFs predicted for a single conjunction's nominal time of closest approach (TCA) and propagated forward and backward from that point in time.

These two BFMC approaches are referred to as "from-epoch" and "from-TCA", respectively.[7]

For each trial, the BFMC algorithm checks if the distance between the two objects becomes less than a threshold hard-body radius miss distance, H, within the risk assessment interval, and, if so, registers a simulated collision at the corresponding time of first contact. This time of first contact is carefully defined and determined[7] such that at most one hit can be registered per trial, thereby avoiding multiple-counting errors that can lead to inflated estimates of risk. BFMC repeats this process for a large number of trials, yielding a best-estimate collision probability of

$$\tilde{P}_c = \tilde{P}_c(\tau_a, \tau_b) = N_c(\tau_a, \tau_b)/N_s \qquad (1)$$

Here τ_a and τ_b denote the beginning and end of the risk assessment interval, N_c the number of hits registered during that interval, and N_s the total number of sampling trials. BFMC also estimates an asymmetric confidence interval for $\tilde{P}_c$ using the Clopper-Pearson method.[11,12]

In the "from-epoch" mode, BFMC samples SP state vectors at the two OD epochs and propagates them throughout the risk assessment interval. SP state vectors include the six equinoctial orbital elements, supplemented by additional state parameters that account for atmospheric drag and solar radiation pressure orbital perturbations.[7-9] BFMC's "from-epoch" mode uses an SP propagation scheme which incorporates the most recent version of the Jacchia-Bowman atmospheric density model[13] plus the associated Dynamic Calibration Atmosphere (DCA) for the High Accuracy Satellite Drag Model (HASDM).[14] This scheme was selected specifically to match the currently operational SP software configuration of the Astrodynamics Support Workstation (ASW).[15,16] Epochs, states, and uncertainty PDFs are derived from *Vector Covariance Messages* (VCMs) produced by the ASW OD processing system. Because VCMs for both the primary and secondary object are used as inputs for the processing, BFMC's "from-epoch" mode is also referred to as "VCM mode."

The "from-TCA" mode differs from the "from-epoch" mode in two fundamental ways.[7] First, it samples equinoctial element state vectors from marginalized PDFs predicted at the conjunction's nominal TCA, as opposed to the OD epochs. Second, it propagates the orbital states using computationally efficient Keplerian 2-body equations of motion. All input data required for "from-TCA" processing can be derived from a single *Conjunction Data Message* (CDM), so BFMC's "from-TCA" mode is also called "CDM mode." Because the CDM mode employs 2-body propagation, it must be restricted to relatively short risk assessment intervals near the conjunction's nominal TCA; 2-body propagation neglects orbital perturbations that can affect satellite motion over extended time scales.[7]

The BFMC Risk Assessment Interval

Coppola[17] formulates a method of estimating the effective duration of a single conjunction, which depends on the relative velocity of the encounter as well as the state uncertainties. BFMC utilizes this duration as a basis for determining a risk assessment interval for temporally-isolated conjunctions.[7] However, for satellites which experience long-duration and/or repeating conjunctions,[6,10,18] the risk assessment interval must be extended. For such cases, BFMC's VCM-mode has been modified to employ a potentially much longer interval (e.g., extending over multiple orbital periods). This modification results in three distinct BFMC simulation modes:

1. CDM mode: "from-TCA" 2-body motion propagations for temporally-isolated conjunctions using short-duration risk assessment intervals based on the Coppola conjunction duration.
2. Short-duration VCM mode (SD-VCM): "from-epoch" SP propagations for temporally-isolated conjunctions using short-duration risk assessment intervals based on the Coppola duration.
3. Long-duration VCM mode (LD-VCM): "from-epoch" SP propagations for long-duration and/or repeating conjunctions using extended (i.e., multi-orbit) risk assessment intervals.

The software modifications described in this analysis extend the BFMC algorithm by fully implementing the third, LD-VCM mode listed above (the first two had been implemented previously[7]). When running LD-VCM mode, the registration of simulated collisions at the time of first contact of the two hard-body spheres is the same as SD-VCM mode; in fact, the only difference between these two modes is the length of the risk assessment interval. Great care has been taken to ensure that times of first contact have been determined accurately in all three BFMC modes.

Identifying Repeating Conjunctions

A repeating conjunction occurs when a set of OD solutions produce multiple close approach events between two objects within a multi-orbit period. However, this broad definition could conceivably include a very large number of interactions between Earth orbiting satellites, depending on what cutoff is used to define a "close approach." This section presents a more rigorous definition of repeating conjunctions, as well as a method to discriminate them from temporally-isolated events.

An SP orbital state is represented by an 8x1 vector, $\boldsymbol{X} = \left[n, a_f, a_g, \chi, \psi, \lambda_M, B, S\right]^T$, with the first six elements denoting the satellite's equinoctial orbital elements, and the last two a ballistic coefficient and a solar radiation pressure parameter.[7,8,19-21] The SP states can be propagated to predict high fidelity satellite position and velocity vectors at time t, denoted symbolically here as $\boldsymbol{r}(t; t_0, \boldsymbol{X}_0, \boldsymbol{\mathcal{D}})$ and $\boldsymbol{v}(t; t_0, \boldsymbol{X}_0, \boldsymbol{\mathcal{D}})$, respectively, where t_0 and $\boldsymbol{X}_0$ represent the time and SP orbital state at epoch, respectively, and $\boldsymbol{\mathcal{D}}$ represents an ensemble of model and environmental data sets required for SP propagation. Similarly, SP mean states and covariances can be propagated[8,19-21] and denoted as $\overline{\boldsymbol{X}}(t; t_0, \overline{\boldsymbol{X}}_0, \boldsymbol{\mathcal{D}})$ and $\boldsymbol{P}(t; t_0, \overline{\boldsymbol{X}}_0, \boldsymbol{P}_0, \boldsymbol{\mathcal{D}})$, respectively. (Note, in this analysis some or all of the function arguments listed to the right of semicolons may be suppressed for brevity.)

The SP epochs, mean states, and covariances for the primary and secondary objects are denoted as:

$$\left(t_{1,0}, \overline{\boldsymbol{X}}_{1,0}, \boldsymbol{P}_{1,0}\right) \qquad \text{and} \qquad \left(t_{2,0}, \overline{\boldsymbol{X}}_{2,0}, \boldsymbol{P}_{2,0}\right) \tag{2}$$

respectively.[7] (This analysis uses subscripts "1" and "2" to indicate quantities associated with the primary and secondary.) BFMC has been modified to propagate mean SP states and covariance matrices for the primary and secondary objects through an extended interval, $\tau_a < t \leq \tau_b$. For the BFMC LD-VCM mode examples discussed in this study, the beginning and end of the risk assessment interval are selected such that

$$\tau_a = \max\left(t_{1,0}, t_{2,0}\right) \qquad \text{and} \qquad \tau_b = \tau_a + 7 \text{ days} \tag{3}$$

However, the BFMC algorithm is not constrained to use these values. For instance, during operational processing, τ_a could be set to a later time if both epochs are several orbital revolutions old (and also to allow time for risk mitigation maneuver planning and execution). Similarly, τ_b could be adjusted on a case-by-case basis to span all high-risk close approach events in a repeating sequence, even if some extend beyond a nominal, pre-specified risk assessment interval.

The time-dependent intervening distance between the mean positions for the primary and secondary objects can be written as

$$r_{2,1}(t) = \left| \boldsymbol{r}_2\big(t; t_{2,0}, \overline{\boldsymbol{X}}_{2,0}\big) - \boldsymbol{r}_1\big(t; t_{1,0}, \overline{\boldsymbol{X}}_{1,0}\big) \right| \tag{4}$$

During a multi-orbit risk assessment interval, $r_{2,1}(t)$ will vary in time as the objects approach and recede from one another. This means that $r_{2,1}(t)$ can have multiple local minima, and the times of these can be defined by imposing three conditions:

$$\boldsymbol{t}_{lmin} = \left\{ \, t \mid \dot{r}_{2,1}(t) = 0 \ \text{ and } \ \ddot{r}_{2,1}(t) > 0 \ \text{ and } \ \tau_a < t \leq \tau_b \, \right\} \tag{5}$$

The first condition requires that the relative velocity, $\dot{r}_{2,1}$, is zero; the second uses the relative acceleration, $\ddot{r}_{2,1}$, to include minima and exclude maxima; the third requires that the minima occur during the risk assessment interval. Each local minimum time in the set $\boldsymbol{t}_{lmin}$ is denoted $t_{lmin,i}$, with $i = 1 \dots N_m$. BFMC calculates position, velocity, and covariance information at each of the minima for both the primary and secondary objects, denoted here as $(\boldsymbol{r}_{1,i}, \boldsymbol{v}_{1,i}, \boldsymbol{P}_{1,i})$ and $(\boldsymbol{r}_{2,i}, \boldsymbol{v}_{2,i}, \boldsymbol{P}_{2,i})$, respectively. These quantities can then be used to calculate a "2D-P_c" semi-analytical collision probability estimate[3,22] for each local minimum, idealizing each as a temporally-isolated conjunction.

The current method implemented in BFMC to identify possible repeating conjunctions can be summarized as follows:

1. Propagate the mean states and associated covariances of both objects throughout the multi-orbit risk assessment interval $\tau_a < t \leq \tau_b$ using high-fidelity SP propagation.

2. Find all local minima of separation distance $r_{2,1}(t)$ throughout the risk assessment interval.

3. Calculate a 2D-P_c estimate for each minimum, treating each as an individual conjunction.

4. Count the number of these 2D-P_c values which exceed a "repeating conjunction detection threshold" of 10^{-10} (a level provisionally adopted for current BFMC analyses). If this count exceeds one, then classify the interaction as a repeating conjunction to be processed using BFMC's LD-VCM mode.
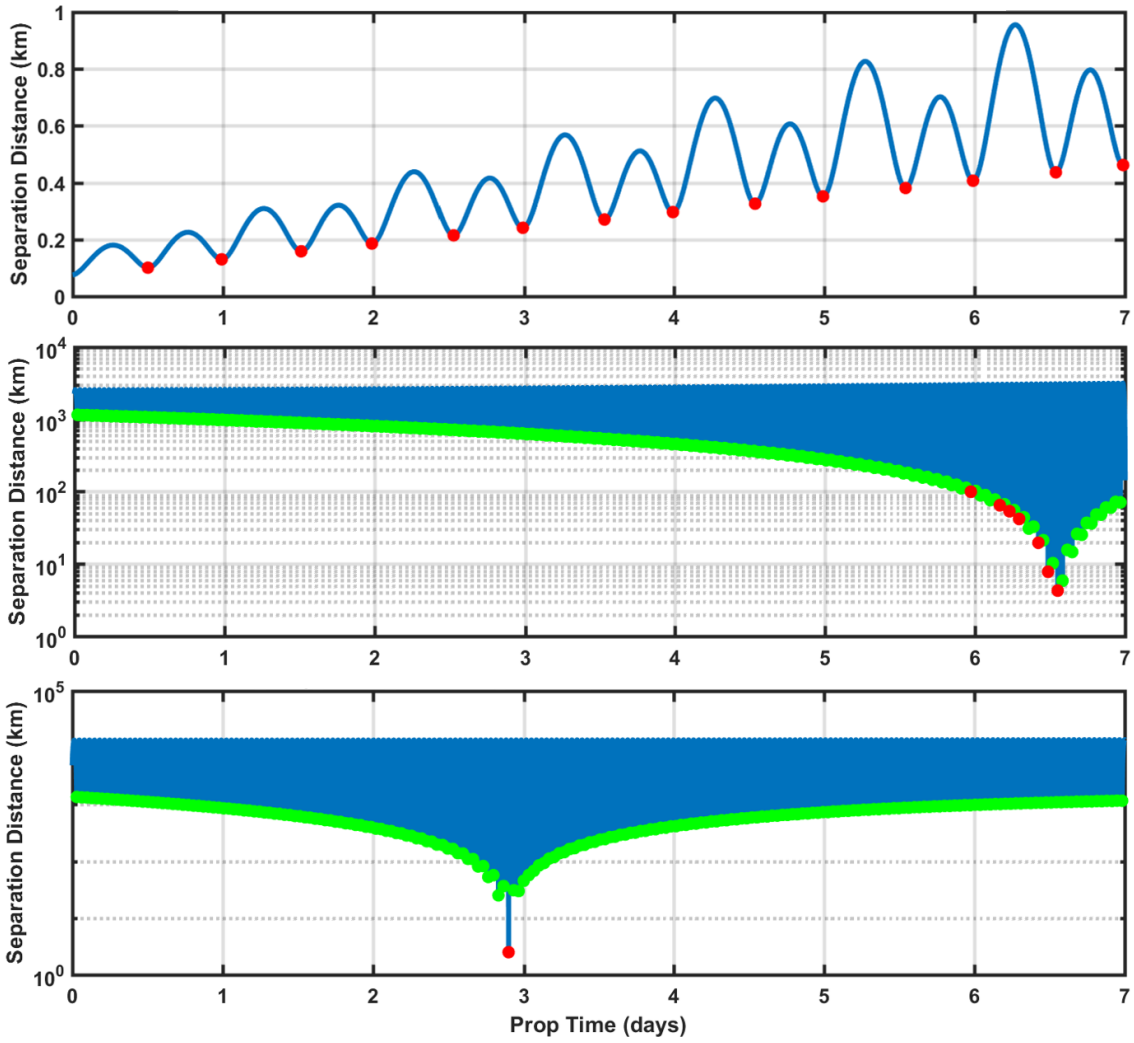
Figure 1: Mean separation distance analysis for a GEO repeating conjunction (top), a LEO repeating conjunction (middle), and a LEO temporally-isolated conjunction (bottom). Red dots indicate single-encounters with 2D-$P_c > 10^{-10}$ and green dots indicate single-encounters with 2D-$P_c \leq 10^{-10}$.

Figure 1 plots mean primary-to-secondary separation distances as a function of time over 7-day risk assessment intervals for three archived example conjunctions, in order to provide a visualization of the repeating conjunction identification process implemented in the BFMC system. This section discusses these separation distance curves in detail; subsequent sections discuss and analyze the corresponding BFMC collision probabilities for all three of these examples.

The top panel of Figure 1 shows a multi-orbit interaction between two coplanar GEO-cluster satellites. During this 7-day interval 14 minima in $r_{2,1}(t)$ occur, at a rate of twice per orbital period. Notably, the 2D-P_c values calculated for each of these minima all exceed the repeating conjunction detection threshold of 10^{-10}. Red dots identify minima with these above-threshold 2D-P_c values, and the occurrence of multiple red dots in the top panel of Figure 1 indicates the detection of a repeating conjunction between these two GEO satellites.

The middle panel of Figure 1 shows an interaction between non-coplanar LEO satellites in which there is a large number of $r_{2,1}(t)$ minima, seven of which have 2D-P_c values that exceed the repeating conjunction detection threshold. Again, the occurrence of multiple red dots in the plot indicates the detection of a repeating conjunction.

The LEO conjunction plotted in the bottom panel of Figure 1, however, contains only one isolated red dot. This indicates that only one of the minima has a 2D-P_c value that exceeds the repeating conjunction detection threshold. In fact, for this interaction all cumulative collision risk during the entire 7-day interval effectively arises from this single encounter. The majority of conjunctions analyzed by CARA can be considered "temporally-isolated" events such as this, in which all risk effectively accumulates during a single close approach during a multi-orbit risk assessment interval. Temporally-isolated conjunctions can be analyzed using either BFMC's CDM mode or SD-VCM mode. Conjunction sequences in which risk accumulates over multiple close events require BFMC's newly-implemented LD-VCM mode, which is the most computationally intensive of the three.

The repeating conjunction detection threshold value of 10^{-10} used in this analysis was tested against a subset of 90 CARA high risk conjunctions. Of these, the identification process outlined above properly identified all six conjunctions for which manual processing indicated that collision risk accumulates during multiple encounters. While these initial results are promising, a more detailed analysis of the specific repeating conjunction threshold value is required.

Assessing a Repeating Conjunction

BFMC's CDM and SD-VCM modes focus on calculating an P_c and an associated P_c confidence interval for a single, temporally-isolated event. BFMC's newly-implemented LD-VCM mode, on the other hand, assesses risks over an extended, multi-orbit interval. This section outlines the method used to identify if and when the cumulative P_c exceeds a threshold that represents the maximum risk tolerable by a satellite operator.

The original BFMC algorithm subdivided the risk assessment interval into evenly-spaced time bins and counted the number of hits occurring within each interval.[7] While this approach worked well for the relatively short duration risk assessment intervals appropriate for temporally-isolated conjunctions, it can become problematic for extended intervals because the algorithm can become complicated and inefficient, due to the extra processing time and memory needed to analyze numerous short-duration bins. For these reasons, the time binning approach used for the original BFMC display software has been replaced by an implementation that determines the cumulative P_c in the form of an empirical cumulative distribution function, based on the exact (not binned) times when hits occur in the simulation. This method works equally well for short-duration and long-duration risk assessment intervals, and eliminates the processing needed to analyze time bins, but retains all of the risk assessment information content produced by the BFMC simulations.

In addition to eliminating the time bins, a burst detection algorithm has been developed to detect groups of closely-spaced hits within the BFMC simulation, summarized as follows. Let N_c be the total number of hits detected by BFMC and $\boldsymbol{t}_c$ be the set of hit times relative to τ_a. The time of the kth hit for $1 \leq k \leq N_{hit}$ is denoted as $t_c(k)$. The orbital period of an object, $\mathcal{P}$, is determined from the object state[8] at epoch. The minimum orbital period is $\mathcal{P}_{min} = \min(\mathcal{P}_1, \mathcal{P}_2)$. A burst, $\boldsymbol{k}_{burst}$, is defined as the set of sequential k indexes such that

$$t_c(k) - t_c(k-1) \leq \frac{\mathcal{P}_{min}}{9} \tag{6}$$

In other words, a burst is a set of hit indexes grouped such that the time separating any two adjacent hits does not exceed 1/9th of the minimum orbital period of the two objects. This burst detection

algorithm is helpful in identifying repeating conjunctions, and recognizing those cases in which the risk from the individual close approach events effectively blends together in time.
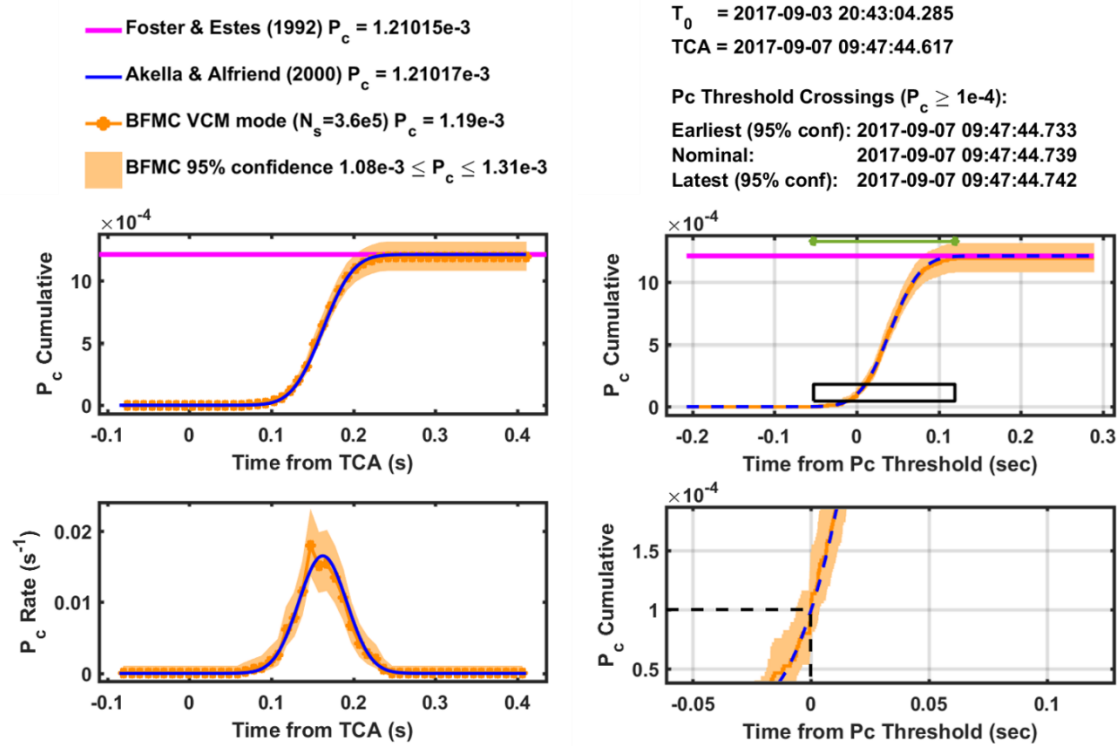

Figure 2: Original BFMC temporal risk plots (left) versus current BFMC plots (right) for a temporally-isolated conjunction between NASA's Aqua satellite and a debris object. The legend for the current BFMC plots has been omitted for brevity, but contains the same information as the legend above the original BFMC outputs.

Figure 2 shows a comparison of graphs generated by the original BFMC implementation (left panels) and the revised, current version (right panels) for an example temporally-isolated conjunction between two LEO satellites. The top plots show the cumulative P_c as a function of time. The orange dots in the original plots on the left represent center-points of the time bins no longer used by BFMC. The original P_c rate plot (bottom-left) has been replaced by an expanded cumulative P_c plot (bottom-right) that zooms in on the time that the cumulative P_c exceeds a maximum risk threshold. This "P_c threshold crossing" represents an estimate of when the collision risk grows beyond a user-specified, maximum tolerable P_c threshold, set to 10^{-4} for this example as shown by the dashed black line. The black box inset on the top-right graph indicates the extent of this zoomed view. The new BFMC implementation changes the horizontal time-axis from measuring "Time from TCA" on the left to "Time from P_c Threshold Crossing" on the right. (Alternatively, this axis can plot "Time Since Latest OD Epoch" as will be shown in later examples.) The new plots additionally include the latest OD epoch time (T_0), the TCA of the conjunction being analyzed (if temporally-isolated), and the nominal P_c threshold crossing time along with an associated 95% estimation confidence interval. Individual bursts of hits detected in the BFMC simulation are indicated with colored segments across the top of the revised cumulative P_c plot; for this temporally-isolated event, the BFMC system detects only a single burst with a duration indicated by the green segment in the top-right plot of Figure 2. For temporally-isolated conjunctions, the current software can also plot 2D-P_c estimates. Specifically, the horizontal pink lines indicate 2D-P_c values calculated using the

Foster and Estes method[3] and the blue lines (solid and dashed) indicate 2D-P_c values calculated using the Akella and Alfriend method.[22]

Example Repeating Conjunctions

The previous section demonstrates how the revised BFMC implementation can display collision risk assessment information for a single, temporally-isolated conjunction. This section demonstrates how information can be displayed for repeating conjunctions, using several examples. As in the previous example, the maximum-risk P_c threshold for all cases has been set to 10^{-4}; this value represents "red" events which often require maneuver planning and execution support by CARA.[23]
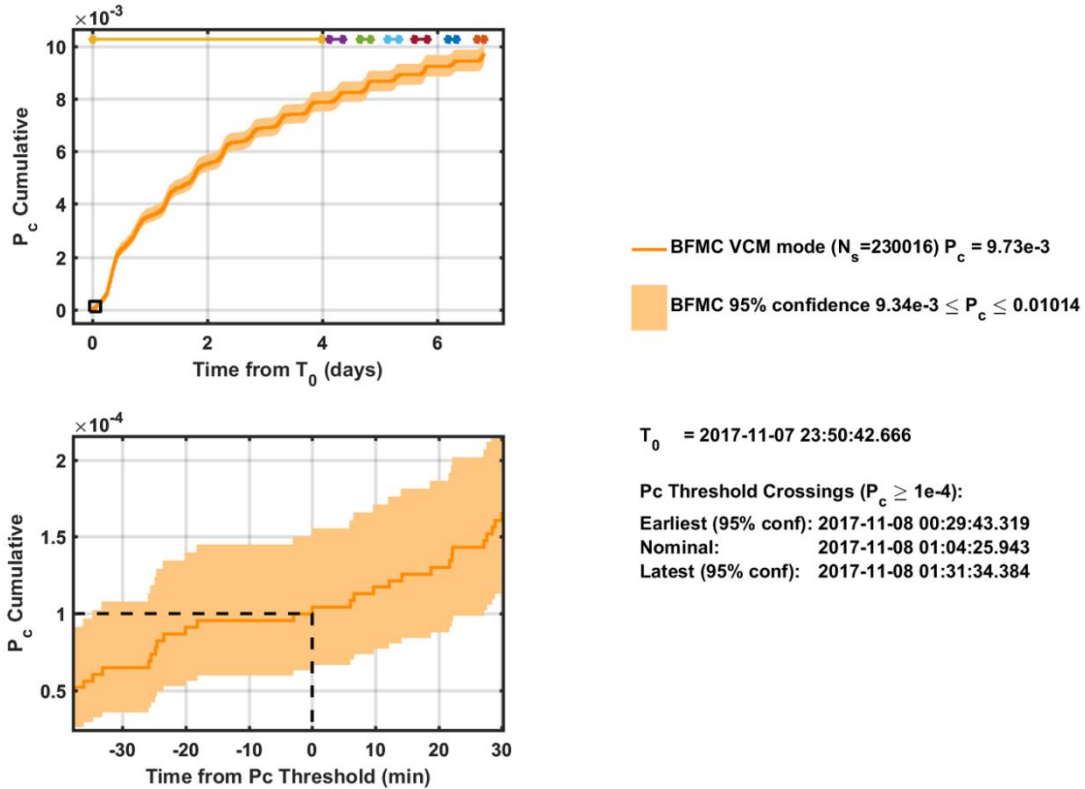

Figure 3: Temporal risk plots for a repeating conjunction between the DIRECTV 12 and DIRECTV 15 GEO cluster satellites using a combined HBR of 10 m.

GEO Repeating Conjunction Example

Figure 3 shows a BFMC risk assessment for a repeating conjunction that occurred in November of 2017 between two closely-spaced, coplanar GEO satellites: DIRECTV 12 and DIRECTV 15. These two active satellites orbit in a tight cluster and experience numerous repeating conjunctions with one another. Figure 3 shows an example 7-day risk assessment for this interaction, beginning at the latest OD epoch time of T_0 = 2017-11-07 23:50:43, and calculated assuming a combined hard-body radius of 10 meters (this HBR does not represent the actual combined sizes of these DIRECTV satellites, and is used here only for illustrative purposes). The top panel of Figure 1 shows the nominal separation distance between these GEO satellites over this period, indicating that 14 close approach events occur during this repeating conjunction interaction at a rate of two per orbital period, as mentioned previously. The stair-step pattern of the cumulative P_c curve in the top plot of Figure 3 shows how risk accumulates as the objects approach and recede from one another. BFMC

indicates that the cumulative P_c grows during the 7-day risk assessment interval up to a final maximum value of $\tilde{P}_c = 9.73 \times 10^{-3}$ with 95% estimation confidence of $9.34 \times 10^{-3} \leq \tilde{P}_c \leq 10.14 \times 10^{-3}$. The colored bars along the top panel of Figure 3 show that the BFMC software detects several bursts of hits during the interval. Notably, the first burst spans four days, indicating that the eight repeating conjunctions that occur during this period have such long individual durations that they effectively blend together in time, leading to a rounded stair-step pattern in this portion of the cumulative P_c curve. Subsequent bursts have shorter spans, indicating shorter effective conjunction durations.

The lower panel of Figure 3 shows the area of interest bounding the P_c threshold crossing. For this example, the cumulative P_c exceeds the maximum-risk threshold of 10^{-4} early during the first day of the risk assessment interval. Specifically, as noted in text on Figure 3, the best-estimate threshold crossing time occurs at 2017-11-08 01:04 (to within a minute), but could conceivably occur about 35 minutes earlier at the 95% confidence estimation level. To avoid collision risk accumulation above the threshold, one of the two GEO satellites would need to perform a risk mitigation maneuver before this time, for this illustrative example.
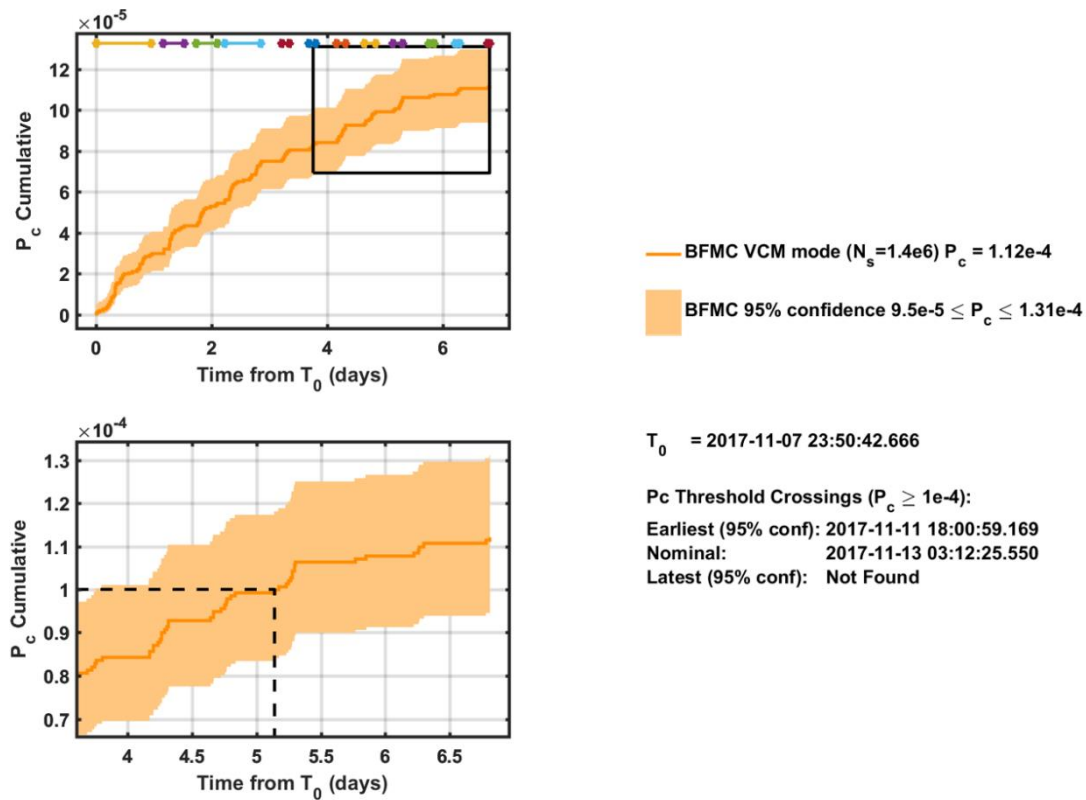

Figure 4: Temporal risk plots for a repeating conjunction between the DIRECTV 12 and DIRECTV 15 GEO satellites using a combined HBR reduced to 1 m.

Cumulative P_c values and threshold crossing times depend on the primary and secondary epoch states and covariances, as well as the HBR value used in the BFMC calculation. To illustrate this, Figure 4 shows a BFMC risk assessment for the same DIRECTV 12 and DIRECTV 15 repeating conjunction interaction discussed above, but with the hard-body radius reduced in the analysis by an order of magnitude, from 10 m down to 1 m. This HBR reduction has the effect of significantly reducing the cumulative P_c estimates, which reach a maximum of $\tilde{P}_c \approx 1.12 \times 10^{-4}$, about two orders of magnitude smaller than in the previous example. The smaller HBR also has the effect of creating

more, better-separated bursts of hits (as marked by the colored bars in the top panel of Figure 4), meaning that the individual conjunctions are less blended in time than in the previous example. Finally, the reduced HBR delays the maximum-risk threshold crossing time by three to five days. Specifically, for this example, the threshold crossing time occurs nominally at 2017-11-13 03:12, but could occur about 33 hours (1.4 days) earlier at the 95% confidence estimation level, as shown in the bottom panel of Figure 4.

LEO Repeating Conjunction

Figure 5 shows a 7-day BFMC risk assessment for a repeating conjunction between non-coplanar LEO satellites that occurred in September of 2017, which differs in nature from the coplanar, closely-spaced GEO examples analyzed above. In this case, BFMC detects three distinct but very brief bursts of hits, marked with the colored dots in the top panel of Figure 5. The middle graph of Figure 1 shows the separation distances between these LEO objects during the risk assessment interval. Note that the close approach events which individually exceed a 2D-P_c threshold of 10^{-10} (marked with red dots in the middle panel of Figure 1) do not necessarily all result in bursts detected in the BFMC simulation.
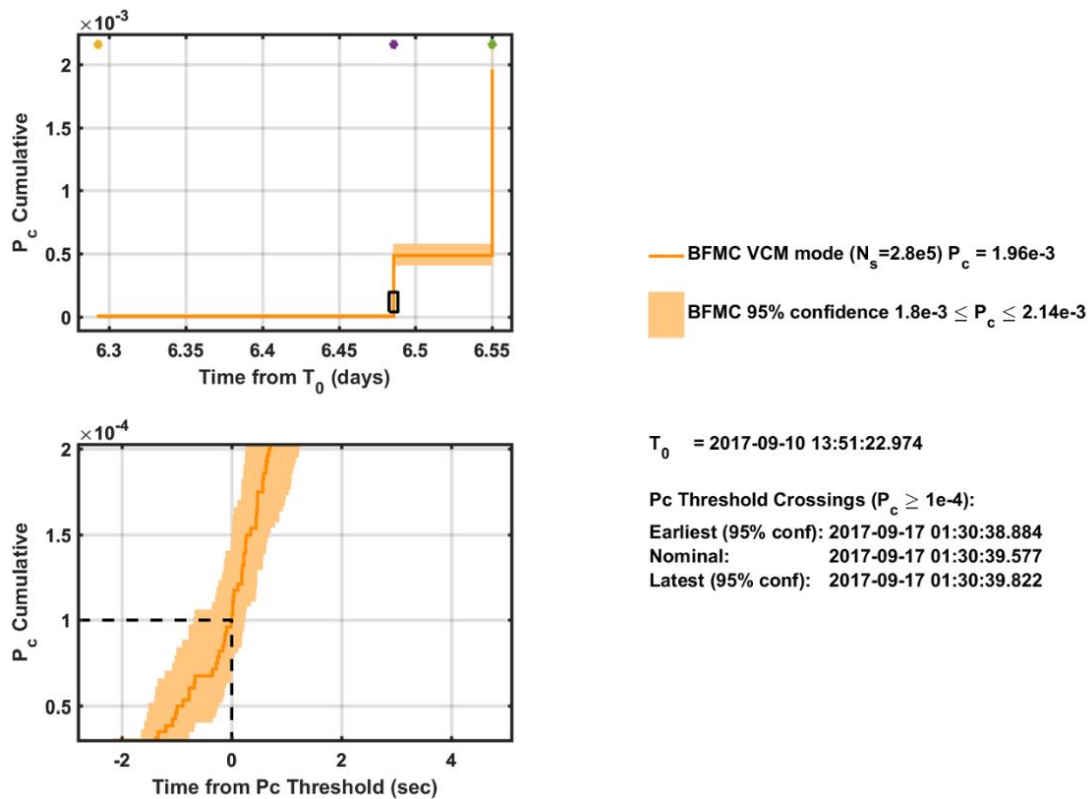

Figure 5: Temporal risk plots for a repeating conjunction between two non-coplanar LEO satellites.

The type of repeating conjunction cumulative P_c plot shown in Figure 5 occurs for interactions between objects in orbits with similar periods, but that are not coplanar (these LEO objects have a relative inclination of ~14°). Such interactions include short bursts of activity (with durations measured in seconds) interspersed between relatively long periods with no hits or significant accumula-

tion of collision probability. This means that the individual close approaches of the repeating sequence all have short conjunction durations, and are well separated in time (rather than blended or nearly blended as in the previous examples).

Figure 5 also illustrates that P_c can accumulate in bursts of unequal amplitude during repeating conjunction sequences, leading to an uneven stair-step pattern in the cumulative P_c curve. Specifically, the first burst (which occurs at $T_0+6.29$ days) has relatively little effect on the overall P_c, but the second burst (at $T_0+6.48$ days) increases it up to $\tilde{P}_c \approx 5\times10^{-4}$, well above the maximum risk threshold. The third burst (at $T_0+6.55$ days) increases it further, to a final estimate of $\tilde{P}_c \approx 2\times10^{-3}$ for the entire 7-day risk assessment period. This highlights the ability of BFMC repeating conjunction analyses to reveal when the most serious encounters occur during multi-orbit risk assessment intervals, in addition to when a maximum tolerable risk threshold will be exceeded.

CONCLUSIONS

The analysis yields the following conclusions:

1. BFMC's CDM and BFMC SD-VCM analysis modes can accurately assess risk for short-duration, temporally-isolated conjunctions. However, BFMC's newly-implemented LD-VCM mode should be used for long-duration and/or repeating conjunction interactions.
2. An initial method for identifying repeating conjunctions can be summarized as follows:
    a. Propagate the mean SP states and covariances of both objects throughout the multi-orbit risk assessment interval.
    b. Find all of the local minima of the primary-to-secondary separation distances for the propagated mean states throughout the risk assessment interval.
    c. Calculate 2D-P_c estimates for each of the minima, treating each as an individual temporally-isolated conjunction.
    d. Count the number of these 2D-P_c values which exceed a (provisional) repeating conjunction detection threshold of 10^{-10}; if there is more than one, then classify the interaction as a repeating conjunction.
3. In addition to the cumulative P_c itself, the maximum-risk P_c threshold crossing time should be used as an additional risk assessment metric for repeating conjunctions. Specifically, to avoid accumulation of collision risk above a maximum tolerable P_c level, a mission must perform a risk mitigation maneuver prior to this threshold crossing time.

This paper presents an update to the BFMC algorithm which allows for the identification and processing of repeating and long-duration conjunctions. An important aspect to repeating conjunction risk assessment is to estimate the time that a maximum-risk P_c threshold is exceeded during the extended, multi-encounter interaction. If this threshold crossing time is not taken into account, a satellite operator analyzing close approach events one at a time may unknowingly delay (or not perform) a risk mitigation maneuver, and put the satellite at elevated risk.

Areas for future research include further tests against repeating conjunctions; the example cases presented in this paper demonstrate the capability of the algorithm but do not rigorously test its overall robustness. Another avenue of research could explore ways to combine multiple, single-encounter 2D-P_c estimates (assuming statistical independence) in order to approximate a consolidated collision probability for a repeating conjunction sequence. Specifically, consolidated 2D-P_c estimates for a large number and variety of repeating conjunction interactions could be compared to the BFMC estimates to assess the effectiveness and limitations of this approach. This consolidated 2D-P_c approach could reduce the computation required for risk analysis significantly by reducing the use of BFMC's slowest LD-VCM simulation mode. As mentioned previously, more

analysis is also needed to determine an optimal P_c threshold level used to identify repeating conjunction events. Finally, the overall challenge remains to identify which conjunctions require BFMC processing, and which specifically require CDM mode, SD-VCM mode, or LD-VCM mode processing.

SYMBOLS AND ACRONYMS

a_f	= the 2$^{\text{nd}}$ equinoctial orbital element, component of the eccentricity vector
a_g	= the 3$^{\text{rd}}$ equinoctial orbital element, component of the eccentricity vector
B	= Ballistic coefficient SP state parameter
$\boldsymbol{D}$	= collected ensemble of model and environmental data sets required for SP propagation
H	= HBR
i	= index for local minima, $i = 1 \dots N_m$
k	= index for MC collisions or hits, $k = 1 \dots N_{hit}$
$\boldsymbol{k}_{burst}$	= set of hit indexes within a single burst
N_c	= the number of MC collisions or hits
$N_c(\tau_a, \tau_b)$	= the number of MC collisions or hits registered during the time interval $\tau_a < t \leq \tau_b$
N_m	= number of local minima
N_s	= the total number of MC sampling trials conducted in a simulation
n	= the 1$^{\text{st}}$ equinoctial orbital element, the mean motion
$\mathcal{P}$	= orbital period
$\mathcal{P}_1$	= orbital period for the primary object
$\mathcal{P}_2$	= orbital period for the secondary object
$\mathcal{P}_{min}$	= minimum orbital period
$\boldsymbol{P}$	= SP state uncertainty covariance matrix
$\boldsymbol{P}_0$	= SP state uncertainty covariance matrix at the OD epoch time
$\boldsymbol{P}_{1,0}$	= SP state uncertainty covariance matrix at the OD epoch time for the primary object
$\boldsymbol{P}_{2,0}$	= SP state uncertainty covariance matrix at the OD epoch time for the secondary object
$\boldsymbol{P}_{1,i}$	= SP state uncertainty covariance matrix at the local minimum at index i for the primary object
$\boldsymbol{P}_{2,i}$	= SP state uncertainty covariance matrix at the local minimum at index i for the secondary object
P_c	= collision probability
$\tilde{P}_c(\tau_a, \tau_b)$	= P_c estimated from an MC simulation for the time interval $\tau_a < t \leq \tau_b$
$\boldsymbol{r}$	= ECI position vector propagated from OD epoch using SP propagation
$\boldsymbol{r}_{1,i}$	= ECI position vector propagated to local minimum at index i for the primary object
$r_{2,1}$	= distance between the primary and secondary objects
$\dot{r}_{2,1}$	= rate of change of the distance between the primary and secondary objects
$\ddot{r}_{2,1}$	= rate of change of the velocity between the primary and secondary objects
$\boldsymbol{r}_{2,i}$	= ECI position vector propagated to local minimum at index i for the secondary object
S	= Solar radiation pressure SP state parameter
T_0	= the latest OD epoch time = $\max(t_{1,0}, t_{2,0})$
t	= time
t_0	= OD epoch time
$t_{1,0}$	= OD epoch time for the primary object
$t_{2,0}$	= OD epoch time for the secondary object
$\boldsymbol{t}_c$	= set of times when hits were detected from an MC simulation
$t_c(k)$	= individual hit time at index k

$\boldsymbol{t}_{lmin}$ = set of times representing the local minima
$t_{lmin,i}$ = time of the local minimum at index i
$\boldsymbol{v}$ = ECI velocity vector propagated from OD epoch using SP propagation
$\boldsymbol{v}_{1,i}$ = ECI velocity vector propagated to local minimum at index i for the primary object
$\boldsymbol{v}_{2,i}$ = ECI velocity vector propagated to local minimum at index i for the secondary object
$\boldsymbol{X}$ = SP state vector
$\boldsymbol{X}_0$ = SP state vector at the OD epoch time
$\overline{\boldsymbol{X}}$ = mean SP state vector
$\overline{\boldsymbol{X}}_0$ = mean SP state vector at the OD epoch time
$\overline{\boldsymbol{X}}_{1,0}$ = mean SP state vector at the OD epoch time for the primary object
$\overline{\boldsymbol{X}}_{2,0}$ = mean SP state vector at the OD epoch time for the secondary object

χ = the 4th equinoctial orbital element, component of the ascending node vector
λ_M = the 6th equinoctial orbital element, the mean longitude
ψ = the 5th equinoctial orbital element, component of the ascending node vector
τ_a = beginning time of a risk assessment interval
τ_b = ending time of a risk assessment interval

2D = two-dimensional
2D-P_c = 2D collision probability
ASW = Astrodynamics Support Workstation
BFMC = Brute Gorce Monte Carlo
CARA = Conjunction Assessment Risk Analysis
CDM = Conjunction Data Message
DCA = Dynamic Calibration Atmosphere
ECI = Earth-Centered Inertial
HASDM = High Accuracy Satellite Drag Model
HBR = Hard Body Radius
LD-VCM = Long-Duration VCM mode
MC = Monte Carlo
NASA = National Aeronautics and Space Administration
OD = Orbit Determination
PDF = Probability Density Function
SD-VCM = Short-Duration VCM mode
SP = Special Perturbations
TCA = Time of Closest Approach
VCM = Vector Covariance Message

REFERENCES

[1] L.K. Newman and M.D. Hejduk, "NASA Conjunction Assessment Organizational Approach and the Associated Determination of Screening Volume Sizes," *International CA Risk Assessment Workshop*, 19-20 May 2015.
[2] B.D. Tapley, B.E. Schutz, and G.H. Born, *Statistical Orbit Determination*, Elsevier Academic Press, Burlington, MA, 2004.
[3] J.L. Foster and H.S. Estes, "A Parametric Analysis of Orbital Debris Collision Probability and Maneuver Rate for Space Vehicles," NASA/JSC-25898, Aug. 1992.
[4] K. Chan, *Spacecraft Collision Probability*, El Segundo, CA, The AeroSpace Corporation, 2008.

[5] S. Alfano, "Satellite Conjunction Monte Carlo Analysis," *AAS SpaceFlight Mechanics Meeting*, Pittsburgh, PA, Paper 09-233, Feb. 2009.

[6] B.M. Braun, "The Evolution of Secondary Object Positions in 18SCS Conjunction Data Messages," *AAS Astrodynamics Specialist Conference*, Columbia Valley, WA, Paper 17-650, 2017

[7] D. T.Hall, S.J. Casali, L.C. Johnson, B.B. Skrehart, and L.G. Baaars, "High Fidelity Collision Probabilities Estimated Using Brute Force Monte Carlo Simulations," *AAS Astrodynamics Specialist Conference*, Snowbird, UT, Paper 18-244, Aug. 2018.

[8] D.A. Vallado, *Fundamentals of Astrodynamics and Applications*, 2rd ed., Microcosm Press, El Segundo CA, 2001.

[9] C. Sabol, C. Binz, A. Segerman, K. Roe, and P.W. Schumacher, Jr., "Probability of Collisions with Special Perturbations using the Monte Carlo Method," *AIAA/AAS Astrodynamics Specialist Conference*, Girdwood, AK, Paper 11-435, Aug. 2011.

[10] D.T. Hall, M.D. Hejduk, and L.C. Johnson, "Time Dependence of Collision Probabilities During Satellite Conjunctions," *AAS/AIAA Space Flight Mechanics Meeting*, San Antonio, TX, Paper 12-271, 2017.

[11] C. Clopper and E.S. Pearson, "The Use of Confidence or Fiducial Limits Illustrated in the Case of the Binomial," *Biometrika*, Vol. 26, pp 404-413, 1934.

[12] N.L. Johnson, S. Kotz, and A.W. Kemp, *Univariate Discrete Distributions*, Wiley-Interscience, Hoboken, NJ, 1993.

[13] B.R. Bowman, W.K. Tobiska, F.A Marcos, C.Y. Huang, C.S. Lin, and W.J. Burke, "A New Empirical Thermospheric Density Model JB2008 Using New Solar and Geomagnetic Indices," *AIAA/AAS Astrodynamics Specialist Conference*, Honolulu, HI, Paper AIAA 2008-6348, 2008.

[14] S.J. Casali and W.N. Barker, "Dynamic Calibration Atmosphere (DCA) for the High Accuracy Satellite Drag Model (HASDM)," *AIAA/AAS Astrodynamics Specialist Conference*, Monterey, CA, Paper AIAA 2002-4888, 2002.

[15] Air Force Space Command, "Astrodynamic Standards Software," http://www.afspc.af.mil, 2018.

[16] National Research Council of the National Academies, "Continuing Kepler's Quest Assessing Air Force Space Command's Astrodynamics Standards," *The National Academies Press*, 2012.

[17] V.T. Coppola, "Evaluating the Short Encounter Assumption of the Probability of Collision Formula," *AAS/AIAA Spaceflight Mechanics Meeting*, Charleston, SC, Paper 12-248, Feb. 2012.

[18] K. Chan, "Hovering Collision Probability," *AAS/AIAA Space Flight Mechanics Meeting*, Williamsburg, VA, Paper 15-234, Jan. 2015.

[19] R.A. Broucke and P.J. Cefola, "On the Equinoctial Orbit Elements," *Celestial Mechanics*, Vol. 5, pp. 303-310, 1972.

[20] D. Vallado, "Covariance Transformation for Satellite Flight Dynamics Operations," *AAS/AIAA Astrodynamics Specialist Conference*, Big Sky, MT, Paper 03-526, 2003.

[21] D. Vallado and S. Alfano, "Updated Analytical Partials for Covariance Transformations and Optimization," *AAS/AIAA Space Flight Mechanics Meeting*, Williamsburg, VA, Paper 15-537, 2015.

[22] M.R. Akella and K.T. Alfriend, "The Probability of Collision Between Space Objects," *Journal of Guidance, Control, and Dynamics*, Vol. 23, No. 5, pp. 769-772, 2000.

[23] L.K. Newman, M.D. Hejduk, and L.C. Johnson, "Operational Implementation of a Pc Uncertainty Construct for Conjunction Assessment Risk Analysis," *AMOS Advanced Maui Optical and Space Surveillance Technologies Conference*, Maui, HI, September 2016.